Appl. Phys. A 49, 459–466 (1989)

Applied Physics A Solids and Surfaces

Exploring Magnetic Properties of Ultrathin Epitaxial Magnetic Structures Using Magneto-Optical Techniques

C. A. Ballentine, R. L. Fink, J. Araya-Pochet, and J. L. Erskine

Department of Physics, University of Texas, Austin, TX 78712, USA

Received 4 February 1989/Accepted 15 June 1989

Abstract. We describe magneto-optic Kerr effect studies of ultrathin Fe and Ni films on single crystal surfaces of Ag and Cu. Monolayer Fe films on Ag(100) exhibit the theoretically predicted spin-orbit anisotropy, but also yield some interesting discrepancies between behavior predicted by Kerr effect and by spin-polarized photoemission experiments. Layer-dependent studies of the magnetic moment of Ni on Ag(111) and Ag(100) suggest sp-d hybridization effects quench the first layer magnetic moment on Ag(111) but not on Ag(100). Temperature dependent studies of thin film magnetization obtained from Kerr effect measurements yield thickness dependent Curie temperatures, and critical exponents for several thin film systems.

PACS: 75.30.Gw, 75.70.Ak, 75.40.Cx

Recent scientific and technical advances have created unprecedented new opportunities for fundamental studies of magnetism and magnetic materials. New methods for materials synthesis based on molecular beam epitaxy (MBE) now permit precise control of the composition and structure of epitaxial layers. Epitaxial growth techniques also offer opportunities to deliberately modify the structure of bulk magnetic materials, i.e., fcc Fe, bcc Ni, and bcc Co can be stabilized on suitable substrates. Magnetic structures of this type are known to exhibit properties that depart from those of naturally occurring bulk materials. The two-dimensionality of ultrathin films is accompanied by different local coordination (number of nearest neighbors) and by electronic coupling to the substrate that also serves as a growth template. These factors alone introduce significant modifications in the magnetic behavior of the films.

Parallel to the developments of MBE and other thin film synthesis techniques has been the continued refinement of structural tools such as low-energy electron diffraction (LEED) and the discovery of new structure sensitive methods for probing properties of substrate surfaces, and the atomic level geometry of surfaces and epitaxial layers. Large scale first principles calculations based on the local spin-density approximation have achieved outstanding success in predicting realistic ground state electronic properties of bulk, surface, and thin-film materials. These calculations have the capability of also predicting magnetic properties including magnetic exchange splitting, as well as the preferred spin direction in thin epitaxial films when spin–orbit effects are included.

The advances in predictive capabilities achieved by large scale calculations and the continued improvements in materials synthesis and characterization techniques have been accompanied by the introduction of new experimental probes of thin film magnetic properties. Spin-polarized photoemission is now experiencing a revolutionary advance based on the increased flux available from magnetic insertion devices (undulators) at electron storage rings [1]. Magneto-optic Kerr effect spectroscopy has recently been refined to a state where it can be used to probe monolayer films [2–4]. Other spin sensitive techniques have evolved including spin-polarized LEED, spin-polarized secondary emission using the high spatial resolution of an electron microscope, and spin-polarized core level spectroscopy.

This paper focuses on the use of the magneto-optic Kerr effect to probe magnetic properties of ultrathin magnetic films. A brief description of the technique

including a discussion of factors that affect the sensitivity is presented first. This discussion is followed by three examples in which the Kerr effect is used to probe magnetic anisotropy, electronic coupling effects involving the substrate, and critical behavior of ultrathin magnetic films near the Curie temperature.

1. Magneto-Optic Kerr Effect

Polarized light reflected from a metallic surface is in general elliptically polarized with the axis of the ellipse rotated in relation to the initial polarization vector. This effect is explained quantitatively by the classical Fresnel reflection formulas. When the metallic surface is ferromagnetic, a small additional rotation and phase shift are introduced. The magnetic contributions to the rotation and phase shift are proportional to the magnetization of the surface (not the applied field) and the effect is known as the magneto-optic Kerr effect (MOKE) [5], and the surface magneto-optic Kerr effect (SMOKE) when applied to ultrathin ($d \ll \lambda$) films.

The microscopic origin of the MOKE is well established [6]. The effect is produced by the spin-orbit interaction which couples the spin component of an electron's wave function to its spatial component. Optical absorption at visible wavelengths occurs as a result of electric dipole transitions that involve the spatial overlap of electron wave functions coupled by optical selection rules. When a material is magnetized, spin-orbit coupling introduces a small magnetic contribution to the optical response that can be used to optically probe magnetic properties. In bulk materials, Kerr rotations and ellipticities are of the order of 10^{-4} rad.

2. Experimental Details

Magneto-optic Kerr effect spectroscopy has *not* been widely used to probe the magnetic properties of ultrathin (1–10 monolayer) films. It is therefore appropriate to describe our particular implementation of the technique and to outline some of the important capabilities that the method offers, based on our initial experiments. Figure 1a displays a side view of our Kerr effect/MBE instrument that illustrates its primary features. The vacuum system incorporates two 8″ diameter flanges, that mount MBE cells, and is pumped by a 400 l/s ion pump and a LN_2 cooled titanium sublimation pump that maintain a typical base pressure of 5×10^{-11} Torr. The preparation chamber features an Auger analyzer that can monitor the sample during MBE growth, and a reverse view LEED system for determining the structure of substrates and of epitaxial films. A sample manipulator provides access to the thin film preparation plane

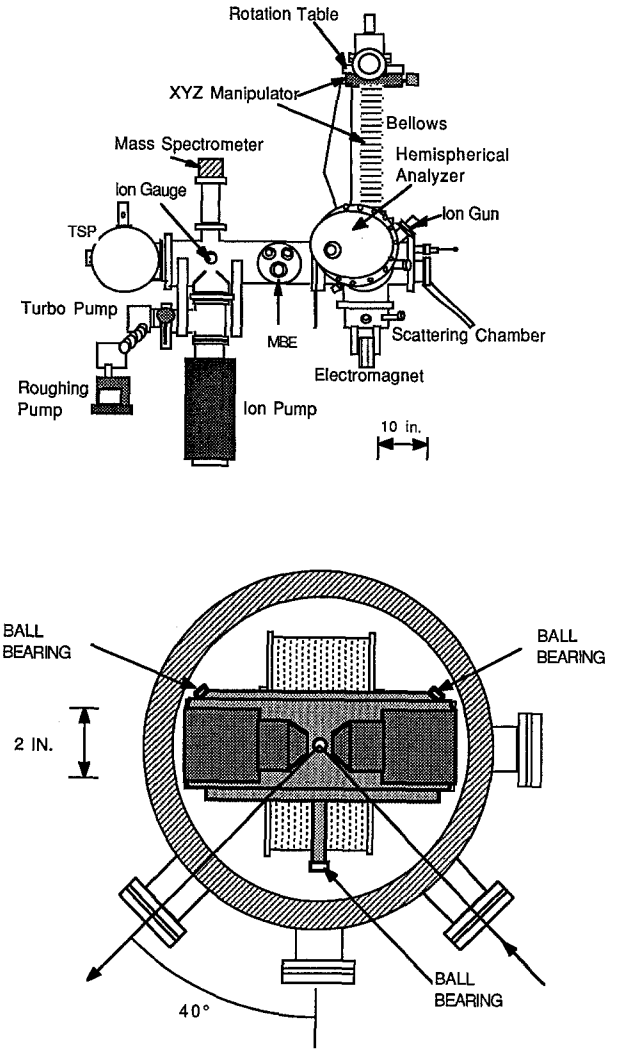

Fig. 1. Upper panel, schematic diagram of the vacuum system that incorporates MBE, LEED/Auger surface analysis, and SMOKE spectroscopy. Lower panel, details of Kerr effect spectrometer part of vacuum system showing rotating magnet pole caps

(LEED/Auger/MBE) and the Kerr effect spectroscopy plane (scattering chamber). Samples can be heated to 2800 °C by electron beam heating and cooled to 100 K (LN_2) or to 30 K (L He). The sample can also be subjected to an applied magnetic field of ± 3000 Oe either in the surface plane or normal to it by a rotatable electromagnet with pole caps inside the vacuum chamber. Details of the scattering chamber are shown in Fig. 1b. Mechanical stability is of paramount importance during Kerr effect measurements. A two-layer thick epitaxial Ni film on Cu(111) yields a Kerr rotation (at $\lambda = 6328$ Å) of approximately 2×10^{-5} rad when magnetized to saturation in the film plane. The entire vacuum system and all optical components, including the source and detectors are mounted on an optical bench that is vibrationally isolated from the

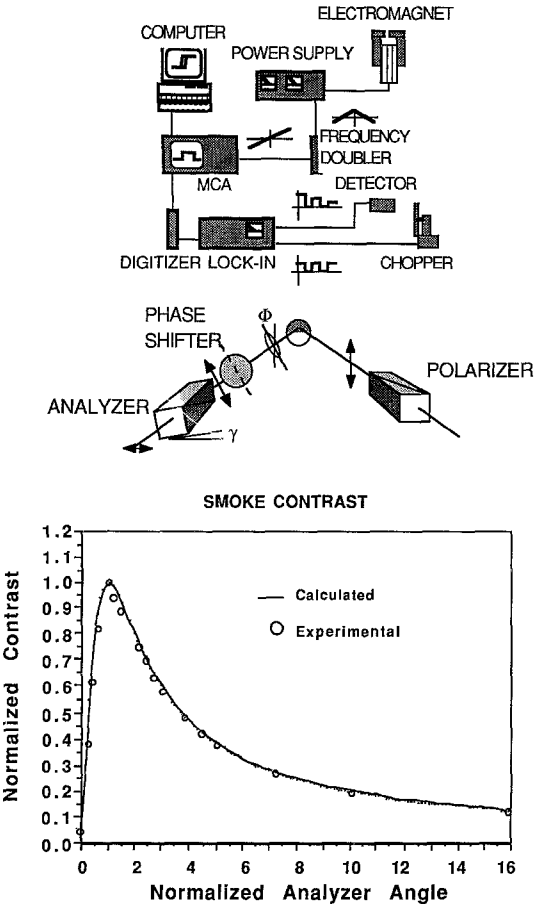

Fig. 2. Upper panel, block diagram of signal processing technique used to measure Kerr effects and obtain hysteresis loops. Optical components are also shown. Lower panel, plot of calculated (line) contrast (refer to text) and experimental measurements showing optimized analyzer angle

floor. Special mechanical stabilization of the dewar is incorporated into the scattering chamber design. Precision laser optical mounts are used throughout.

Figure 2a illustrates the principal optical elements of our Kerr effect spectrometer, and describes the signal processing technique utilized to obtain hysteresis loops from the Kerr rotations. A light beam from a laser or monochromator is chopped and polarized before being reflected from the sample. We usually grow the epitaxial magnetic layers on only half of the substrate to maintain a "reference" surface. Reflected light passes through an optical phase shifter that is adjusted to compensate phase shifts in the reflected beam, and then through an analyzer that converts the polarization rotation $\Delta\phi$ into a change in detected intensity, ΔI. The computer is necessary to account for electromagnet hysteresis effects (table look-up) and for background subtractions.

A straight-forward calculation shows that the contrast C defined by $\Delta I/I_0$, where ΔI is produced by the (Kerr) rotation and I_0 is the transmitted intensity (resulting from depolarization effects and any offset of the analyzer from a crossed position) is given by:

$$C = \frac{2(\gamma/\gamma_m)}{1+(\gamma/\gamma_m)^2}\frac{\phi}{\sqrt{\varepsilon}},$$

where γ is the analyzer angle, and γ_m is the angle that yields the maximum contrast. The angle ϕ is the Kerr effect angle, and ε characterizes the extinction ratio of the optical system (polarizers, windows, and sample surface all included). The extinction ratio can be considered the parameter that governs the performance of the polarimeter. Figure 2b shows a plot of C/C_m (where $C_m = \phi/\sqrt{\varepsilon}$) vs γ/γ_m along with measured values obtained using a three monolayer Fe film on Ag(100). The excellent agreement between experimental results and the analytical expression demonstrates our analysis of the experimental factors affecting the sensitivity of this technique is basically correct.

3. Thin Film Anisotropies, Coercive Forces

It is an experimental fact that (bulk) ferromagnetic single crystals exhibit "easy" and "hard" directions of magnetization; i.e., the energy required to polarize the spins depends on the direction of the applied field relative to the crystal axis. This property (magnetic anisotropy) along with other properties including the coercive force and remanent magnetization are among the most technologically important properties of magnetic materials. It is these properties that provide the basis for information storage and retrieval and other important applications of magnetic materials. Thin film magnetic materials also exhibit magnetic anisotropy. However, the physical basis that underlies a preferred spin orientation in an ultrathin film can be quite different from the factors that account for easy axis alignment along a high-symmetry direction of a single crystal bulk material.

We have recently demonstrated the capability of Kerr effect spectroscopy to probe the magnetic anisotropy of an epitaxial monolayer film [3]. Figure 3 displays layer dependent hysteresis curves obtained from a p(1 × 1) Fe layer on Ag(100). The three upper panels correspond to different directions of the applied magnetic field. From these data, it is clear that the easy axis at $n=1$ layer is perpendicular to the surface, and for $n>2$ layers, the easy axis lies in the plane. The small hysteresis seen in the 2.5 layer film with the applied field perpendicular to the plane is actually due to an in-plane component of magnetization. The in-plane magnetization is reversed by a small longitudinal field caused by slight misalignment of the sample-magnet combination. Subtraction of the in-plane signal results

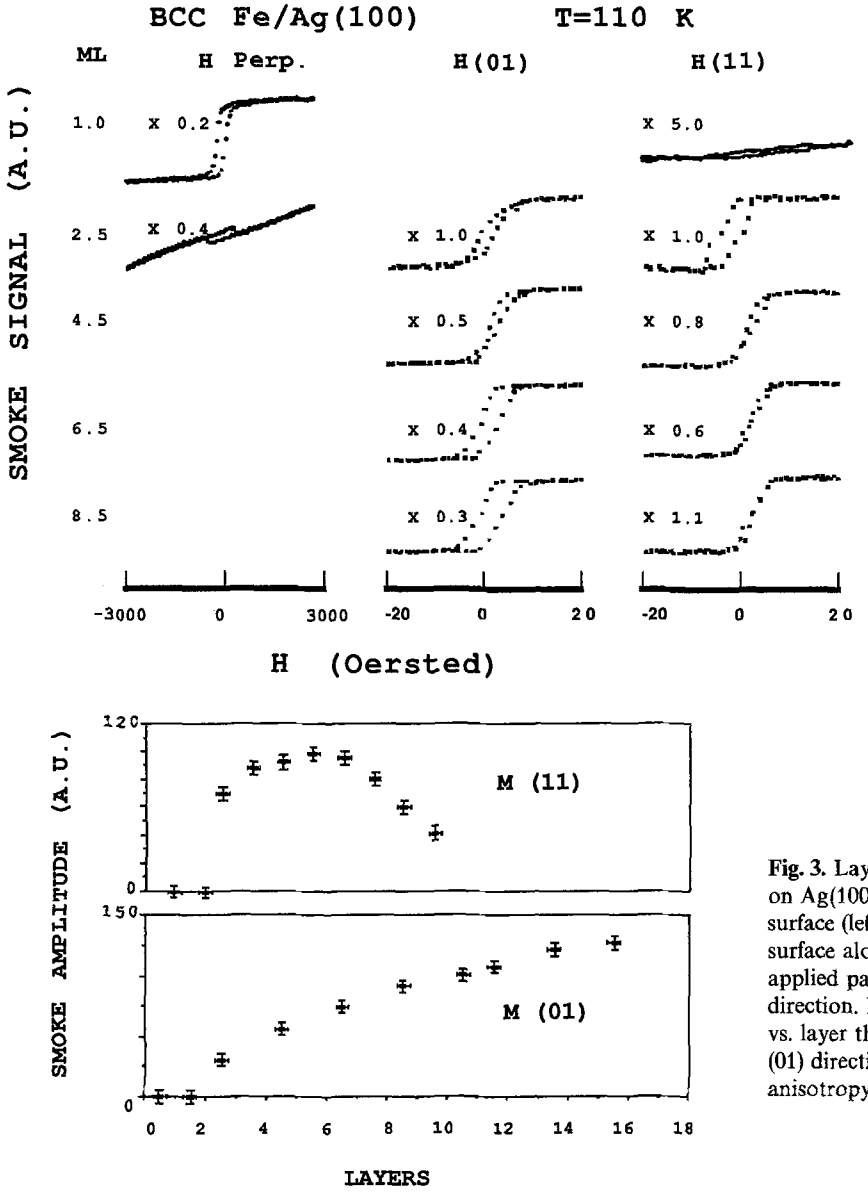

Fig. 3. Layer dependent hysteresis curves for bcc Fe on Ag(100) for H applied perpendicular to the surface (left column), H applied parallel to the surface along a (01) direction (center panel), and H applied parallel to the surface along a (11) direction. Lower panels, plot of SMOKE amplitude vs. layer thickness for M along (11) and M along (01) directions showing evidence of in-plane surface anisotropy

in the linear (hard axis) hysteresis behavior. This data supports the calculations of Gay and Richter [7] that predict spin-orbit effects favor perpendicular spin orientation for a Fe monolayer on Ag(100). The two lower panels of Fig. 3 display layer dependent hysteresis data for applied magnetic fields in the plane and along two inequivalent symmetry directions of a $p(1 \times 1)$ Fe crystal on Ag(100). These results clearly exhibit experimental evidence for in-plane surface magnetic anisotropy. The results also demonstrate the capability of Kerr effect studies of monolayer epitaxial films to yield information about coercive forces, easy and hard directions of magnetization, magnetic remanence and $M(H)$ curves.

It is interesting to note that the spin-polarized results of Stampanoni et al. [8] for Fe on Ag(100) have been interpreted to indicate that the perpendicular anisotropy at 30 K does not persist below 3.5 monolayers, or above 5 monolayers, and that above 100 K there is no perpendicular remanence for any film thickness. Our results suggest that at 100 K the easy direction is perpendicular to the plane for films less than approximately 2.0 monolayers thick and in-plane for films greater than 2 layers. As the temperature is decreased to 30 K we find that films up to 3.0 monolayers thick exhibit a perpendicular easy direction of magnetization. The films thicker than 3.0 layers show evidence that at even lower temperatures they too would have an easy direction perpendicular to the plane. All of our results agree very well with the results from spin-polarized photoemission [9], ferromagnetic resonance (FMR) [10], conversion electron Moss-

bauer spectroscopy (CEMS) [11], and scanning electron microscopy images [12].

The disagreement with the spin-polarized results of Stampanoni is probably due to microstructural differences in the substrates which are used as a template for the thin film overlayers. It has been seen that an increased step density will decrease the perpendicular anisotropy [13]. If their substrate had a high step density, it would take about 3 layers to smooth out these steps and they could then detect the perpendicular anisotropy when the sample is at 30 K. It must be noted though that the CEMS and FMR measurements are made on superlattices and overcoated samples; the photoemission, scanning electron microscopy, and MOKE measurements are done on as grown single film samples and since the extra metal-metal interface may enhance the perpendicular anisotropy, direct comparison of all of these results is difficult.

4. Electronic Structure Effects

Ultrathin epitaxial magnetic films must be grown on substrates. The substrate not only provides a growth template for the film epitaxy, it also can influence the magnetic properties of the film by electronic coupling effects such as charge transfer and sp-d hybridization between electronic states of the film and substrate. These effects have been explored theoretically based on first principles electronic structure calculations. Work by Freeman's group [14] has predicted enhanced moments that depend on specific details of the systems. Corresponding work by Tersoff and Falicov [15] has explored the crucial role sp-d hybridization plays in governing the magnetic properties of ultrathin films. Their results include specific predictions [quenching of ferromagnetic behavior at a Ni/Cu(111) interface] that we have explored using Kerr effect spectroscopy, which is described below.

Figure 4 displays hysteresis curves obtained from Kerr effect measurements of epitaxial Ni films on Ag(111) and Ag(100). The Ni/Ag(111) system exhibits particularly good epitaxy for $n<10$ judged from our LEED observations. We have studied Kerr effects with applied fields (to 3000 Oe) parallel and perpendicular to the surface at a temperature of 110 K. Our results establish that over this range of parameters, the magnetic moment of Ni lies in the plane for both

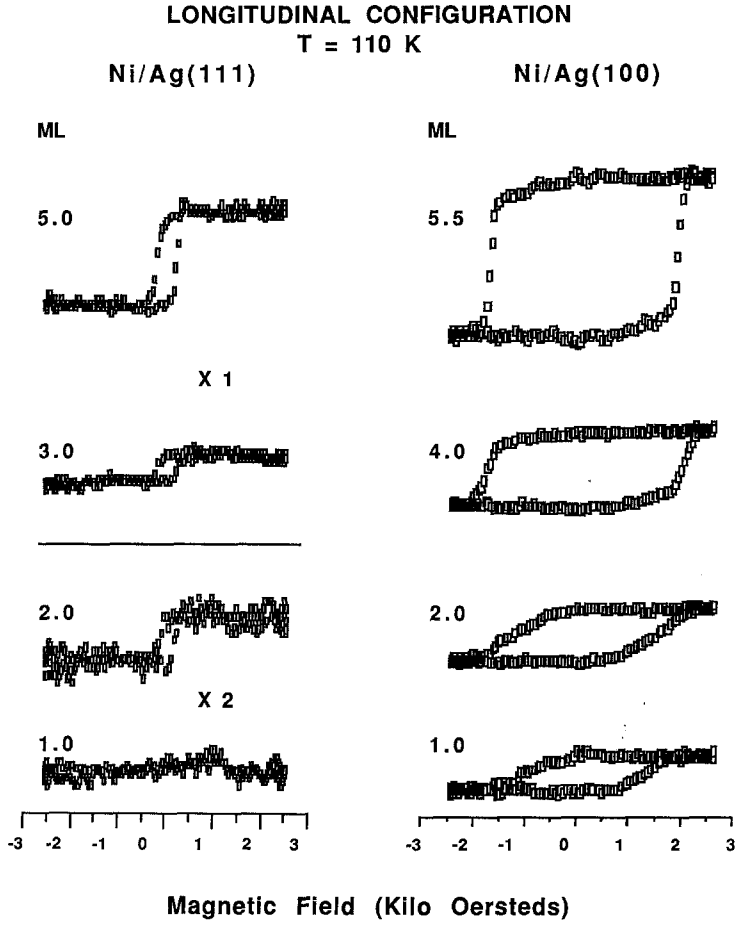

Fig. 4. Hysteresis curves for Ni films on Ag(111) and Ag(100) as a function of thickness. The magnetization appears to be quenched for $n=1$ layer for the Ni/Ag(111) system. The large coersive force for Ni on Ag(100) may be due to the absence of excellent epitaxy which occurs on the Ag(111) surface

Ag(111) and Ag(100) substrates, and that for $n=1$, the moment vanishes on Ag(111) (or is less than 15% of the extrapolated value for $n=1$ based on thicker films). Additional studies at lower temperatures and lower applied fields ($T\sim 40$ K, $H=600$ Oe) have established that the rapid quenching of the Ni film magnetism on Ag(111) is not a consequence of the thickness dependent Curie temperatures. This result suggests the existence of a Ni dead layer or a layer having strongly quenched ferromagnetic moments on Ag(111), but not on Ag(100). Our corresponding studies of Ni on Cu(111) have shown that, as in the case of Ni on Ag, the magnetic moment lies in the plane of the film for the same range of thickness and temperature. The p(1 × 1) Ni film on Cu(111) also exhibits good epitaxy, as judged from our LEED observations and from fairly extensive LEED structural analysis by Tear and Roll [16]. However, there is no apparent quenching of the Ni magnetic moment for $n=1$ on Cu(111) surfaces. This result is consistent with recent photoemission and inverse photoemission studies by Frank et al. [17] that suggest also that a p(1 × 1) Ni layer on Cu(111) is not magnetically "dead". Since we have found that a monolayer film of Ni on Cu(111) is magnetic, Tersoff and Falicov's specific predictions pertaining to the Ni film magnetic moment on Cu(111) appear to be incorrect; however, the general concept of sp-d induced quenching could still account for the behavior that we observe for p(1 × 1) Ni layers on Ag(111).

5. Magnetic Phase Transformations

Ultrathin epitaxial magnetic films provide an important arena for exploring fundamental concepts of statistical mechanics, specifically the magnetic phase transformation in a system that is constrained to two dimensions. The required experimental constraints are clear: the films must be well characterized two dimensional epitaxial structures, and the crystal structure must be preserved as the temperature is varied through the magnetic phase transformation. High sensitivity is required by the magnetic probe because the signal vanishes as T approaches T_c, i.e., in the temperature range of greatest interest. We have shown that such experiments are feasible based on Kerr effect measurements. Several systems have already been identified that appear to satisfy the experimental constraints. We have found that the Curie temperature of a Ni monolayer on Cu(111) is ≈ 175 K, and that ultrathin Ni films grown on Cu(111) yield repeatable Auger and Kerr effect signals after temperature excursions above 100°C. Figure 5 displays curves that characterize the temperature and layer dependence of the magnetization of thin epitaxial Ni films on Cu(111) as determined by Kerr effect signals.

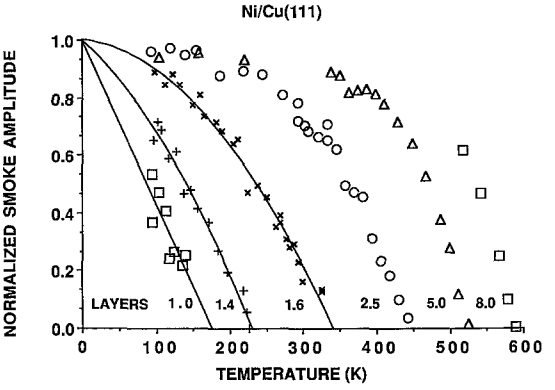

Fig. 5. Temperature and thickness dependent magnetization of epitaxial Ni layers on Cu(111). Note the striking dependence of Curie temperature on film thickness

The data displayed in Fig. 5 can be reduced to obtain parameters relevant to scaling theories for two dimensional phase transformations. Analytical treatments [18] of the magnetic phase transformation predict that the magnetism approaches zero according to a simple power law $M\propto(T-T_c)^{\beta}$ characterized by the transition temperature T_c and a critical exponent β. The thickness dependence of the Curie temperature has also been analyzed and found to obey a power law described by [19]

$$\frac{T_{cb}-T_c(n)}{T_c(n)}=C_0 n^{-\lambda},$$

where T_{cb} characterizes the bulk transition temperature (627 K for Ni). C_0 is a constant having a calculated value of 0.196, and λ is a shift exponent that ranges from 1.0 for free surface boundary conditions to 2.0 ± 0.1 for periodic boundary conditions.

Figure 6 displays a plot of the reduced transition temperature vs. layer thickness for epitaxial Ni films on Cu(111). The inset table summarizes the values of C_0 and λ obtained from these results (obtained from Kerr effect studies) as well as by others for different substrates. Our results yield a shift exponent $\lambda=1.48$ (which lies between the theoretical predictions) that is in good agreement with other experimental values [20–22]. It is interesting to note that Ni/Cu(111) and Ni/Re(0001) [19] are both good epitaxial systems, and that the values of C_0 and λ for these different systems agree within experimental error.

The temperature dependent magnetization data of Fig. 5 can also be used to obtain the critical exponent β. Theoretical values for β are model dependent. An exact value $\beta=1/8$ has been obtained for the two-dimensional Ising model [23]. Other calculations yield values of β including $\beta=1/2$ (by McCoy and Wu [24]

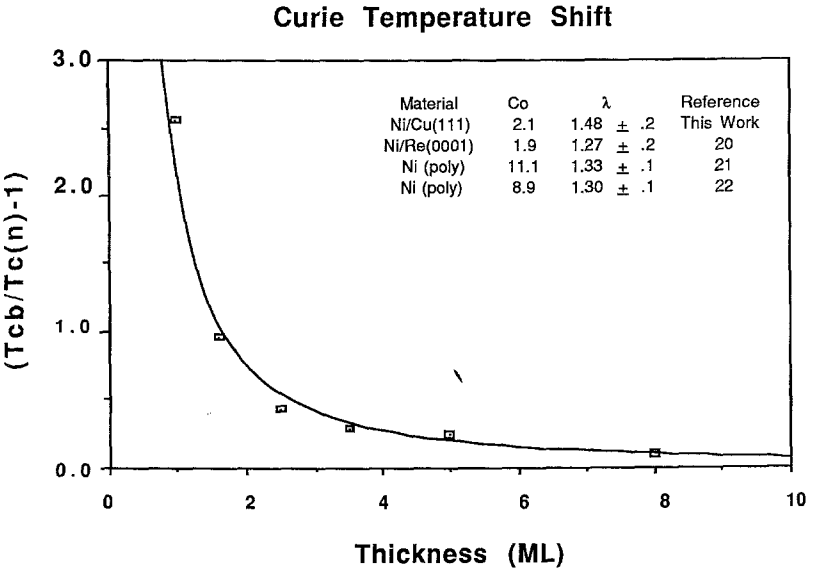

Fig. 6. Plot of the reduced Curie temperature as a function of temperature, (points) and comparison with the scaling power law equation by Ritchie and Fisher. The scaling parameters Co and λ are defined in the text

for a two-dimensional Ising lattice with a one-dimensional free surface), and $2/3 \leqq \beta \leqq 1$ (based on models that treat the surface layer of a bulk crystal by considering distinct values for the surface and exchange energy [18]). Clearly, any comparison of experimental results with a theoretical prediction for β must be based on specific details of the system being studied. With this in mind, we present our results for β corresponding to an epitaxial p(1 × 1) Ni film on Cu(111).

Figure 7 displays a plot of $\log M$ as a function of $\log(1 - T/T_c)$ for 1.6 layers, upper panel, and (5 layers), lower panel, Ni films on Cu(111). The slope of this curve yields the parameter $\beta = 0.56 \pm 0.05$ ($\beta = 0.50 \pm 0.02$). The temperature range covered by our present data corresponds to $0.2 \leqq 1 - T/T_c \leqq 0.5$. Although all experimental points fall nicely on a straight line in this range, it is important to point out that the most relevant temperature range is near T_c. It is not inconceivable that "cross over" behavior could occur at lower temperatures, in which case the slope of the line could change yielding a different exponent. However, based on Rau's results [25] for a V(100) monolayer on Ag(100) covering $2 \times 10^{-4} \leqq (1 - T/T_c) \leqq 0.8$, no significant cross over effects are apparent in this system, and the exponent that we obtain is likely to be quite accurate. The sensitivity of our technique is now being improved, and we expect to extend the reduced temperature range to $0.002 \leqq 1 - T/T_c \leqq 0.8$ to verify the result. It is interesting to note that Rau [25] obtains $\beta_1 = 0.128 \pm 0.01$ for V on Ag(100) and Pescia and Grunberg [26] obtain $\beta = 0.22 \pm 0.05$ for Fe on Au(100). These values for β are closer to the exact theoretical result for a two-dimensional Ising model ($\beta = 1/8$).

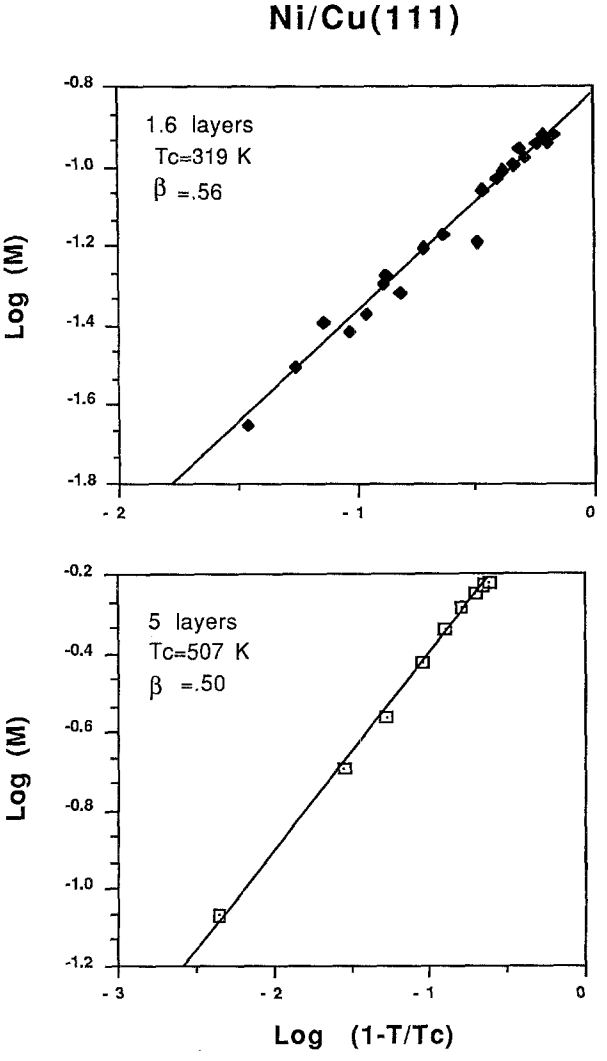

Fig. 7. Critical exponent β for epitaxial Ni films on Cu(111). The parameter β is defined in the text

6. Summary

Several examples consisting of epitaxial ferromagnet layers on non-magnetic metal substrates have been used to describe phenomena associated with thin films that can be addressed using the magneto-optic Kerr effect. The Kerr effect technique offers the capability to probe magnetic anisotropy – both in-plane effects and the novel perpendicular spin orientations that are predicted to occur in very thin layers when the volume-dependent shape anisotropy term becomes small. Layer dependent moments can be probed based on the assumption that optical resonance effects do not occur (i.e., film thickness $\ll 100$ Å). Finally, the sensitivity of the technique can be extended to a point where critical exponents and phase transformations can be studied. Opportunities for exploiting the Kerr effect as a probe of thin film magnetism are clearly very attractive, and are just beginning to be explored.

Acknowledgement. This work was sponsored by the National Science Foundation, under Grants No. DMR-87-02848, DMR-86-03304, and the Joint Services Electronics Program AFOSR-F49620-86-0045.

References

1. P.D. Johnson, A. Clarke, N.B. Brookes, S.L. Hulbert, B. Sinkovic, N.V. Smith: Phys. Rev. Lett. **61**, 2257 (1988)
2. C. Liu, E.R. Moog, S.D. Bader: Phys. Rev. Lett. **60**, 2422 (1988)
   S.D. Bader, E.R. Moog: J. Appl. Phys. **61**, 3729 (1987)
3. J. Araya-Pochet, C.A. Ballentine, J.L. Erskine: Phys. Rev. B **38**, 7846 (1988)
4. T. Beier, H. Jahrreiss, D. Pescia, Th. Woike, W. Gudat: Phys. Rev. Lett. **61**, 1875 (1988)
5. A.V. Sokolov: *Optical Properties of Metals* (Elsevier, New York 1967)
6. P.N. Argyres: Phys. Rev. **97**, 334 (1955)
   B.R. Cooper: Phys. Rev. **139**, A1504 (1965)
   H.S. Bennett, E.A. Stern: Phys. Rev. **137**, A448 (1965)
7. J.G. Gay, R. Richter: Phys. Rev. Lett. **56**, 2728 (1986); J. Appl. Phys. **61**, 3362 (1987)
8. M. Stampanoni, A. Vaterlaus, M. Aeschlimann, P. Meier: Phys. Rev. Lett. **59**, 2483 (1987)
9. B.T. Jonker, K.H. Walker, E. Kisker, G.A. Prinz, C. Carbone: Phys. Rev. Lett. **57**, 142 (1986)
10. B. Heinrech, K.B. Urquhart, A.S. Arrott, J.F. Cochran, K. Myrtle, S.T. Purcell: Phys. Rev. Lett. **59**, 1756 (1987)
11. N.C. Koon, B.T. Jonker, F.A. Volkering, J.J. Krebs, G.A. Prinz: Phys. Rev. Lett. **59**, 2463 (1987)
12. J.L. Robins, R.J. Celotta, J. Urguris, D.T. Pierce: Appl. Phys. Lett. **52**, 1918 (1988)
13. G. Lugert, G. Bayreuther: Phys. Rev. B **38**, 11068 (1988)
14. C.L. Fu, A.J. Freeman, T. Oguchi: Phys. Rev. Lett. **54**, 2700 (1985)
    A.J. Freeman, C.L. Fu: J. Appl. Phys. **61**, 3356 (1987)
15. J. Tersoff, L.M. Falicov: Phys. Rev. B **26**, 6186 (1982)
16. S.P. Tear, K. Roll: J. Phys. C **15**, 5521 (1982)
17. K.H. Frank, R. Dudde, H.J. Sagner, W. Eberhardt: Phys. Rev. B **39**, 940 (1989)
18. K. Binder, P.C. Hohenberg: IEEE Trans. Magnetics **12**, 66 (1976); Phys. Rev. B **9**, 2194 (1974); B **6**, 3461 (1972). Also, see K. Binder: In *Phase Transitions and Critical Phenomena*, ed. by C. Domb, J.L. Leboitz (Academic, New York 1983)
19. D.S. Ritchie, M.E. Fisher: Phys. Rev. B **7**, 480 (1973)
20. R. Bergholz, V. Gradmann: J. Magn. Magn. Mat. **45**, 389 (1984)
21. H. Lutz, J.D. Gunton, H.K. Schumann, J. Aron, T. Mihalisn: Solid State Commun. **14**, 1075 (1974)
22. J. Araya-Pochet, H. Merlos: Cien y Tecn. **5**, 15 (1981)
23. L. Onsager: Nuovo Cimento Suppl. **6**, 261 (1949)
    C.N. Yang: Phys. Rev. **85**, 808 (1952)
24. B.M. McCoy, T.T. Wu: Phys. Rev. **162**, 436 (1967)
25. C. Rau, G. Xing, M. Robert: J. Vac. Sci. Technol. A **6**, 579 (1988)
26. D. Pescia, P. Grunberg: IFF-Bulletin **33** (1988)